Available online at www.sciencedirect.com

ScienceDirect

Procedia Structural Integrity 33 (2021) 320–329

Structural Integrity Procedia

www.elsevier.com/locate/procedia

IGF26 - 26th International Conference on Fracture and Structural Integrity

Simulation of crack growth in T-welded joints - residual stress field effect

Ramalho, A.L.[a,b,*], Antunes, F.V.[b], Ferreira, J.A.M. [b]

[a]*Polytechnic Institute of Castelo Branco, 6000-767 Castelo Branco, Portugal*
[b] *Centre for Mechanical Engineering, Materials and Processes (CEMMPRE), Univ Coimbra, 3004-516 Coimbra, Portugal*

Abstract

In this article, a three-dimensional finite element model is used to predict the growth of cracks at the weld toe of a T-joint. The model is developed using the MSC Marc software. Fatigue life is estimated by integrating the Paris-Erdogan law and the stress intensity factors are obtained by the virtual crack closure technique.
The influence of residual stresses generated by plastic deformation at the weld toe on the crack propagation speed is analyzed. The existence of residual compression stress fields causes a delay in crack growth. The obtained results are compared with the integration solutions of the Paris-Erdogan law using the stress intensity factor computed through the Mk factor proposed by Bowness and Lee, included in BS 7910 standard.

Keywords: Residual stresses; T-welded joints; fatigue crack growth; FEM

1. Introduction

The residual stresses affect fatigue life, therefore must be included in design. Tensile residual stresses reduce fatigue life while compressive residual stresses extend fatigue life. Compressive residual stresses may be introduced

* Corresponding author.
E-mail address: aramalho@ipcb.pt

2452-3216
10.1016/j.prostr.2021.10.039

intentionally in the components using shot peening, Wang et al. (1998), hammer peening, indentation, Ruzek et al. (2012), laser shock peening, Bikdeloo et al. (2020), cold expansion, Lacarac et al. (2000), Giglio and Lodi (2009), overloading or bending plastic deformation, Garcia et al. (2016), Surface Mechanical Attrition Treatment (SMAT) Shreyas and Trishul (2014). On the other hand, the residual stresses may be introduced unintentionally by the technological process, namely by quenching, welding, casting or additive manufacturing.

The presence of cracks at the weld toe, influenced by the effect of stress concentration and residual stresses existing in the area, affects the fatigue life of welded joints. The effect of residual stresses on crack propagation of welded joints has been studied by several authors, Ramalho et al. (2020) and Barsoum and Barsoum (2009).

The virtual crack closure technique (VCCT) allows considering the effect of stress fields in the determination of stress intensity factors, Ramalho et al. (2020). This technique is suitable to estimate the propagation of cracks in three-dimensional finite element models (FEM), Krueger (2004) and Zhao et al. (2020). Although many studies have been published regarding the use of this technique in 2D models, studies regarding 3D models are very limited, use simplified geometries and sometimes require changes to the original VCCT, Okada et al. (2005), Zeng et al. (2016) and Zhao et al. (2020).

The application of this technique in 3D models is mainly limited by the characteristics of the mesh needed to optimize the accuracy of the calculation of stress intensity factors. The mesh must be refined at the crack tip, Kurguzov (2016) and it is also desirable to have some mesh orthogonality in this region, Okada et al. (2005). The use of automatic crack growth algorithms, usually requires remeshing techniques, being conditioned by the geometry and order of the elements. In the case of the MSC Marc software, first-order tetrahedral elements must be used, so for an adequate simulation of the stress and deformation fields at the tip of the crack, an adequate mesh refinement in this area is necessary, Marc (2018). The refinement required in this method requires a high computational and storage effort, being necessary the use of parallel processing in many of the models.

In this paper is presented a 3D finite element method (FEM) model that allows the evaluation of the influence of residual stress fields, generated by overloads, on the propagation of cracks at the toe of T-welded joints.

2. Numerical model

The 2D model previously presented by the authors in Ramalho et al. (2020), is expanded here to 3D. In order to limit the number of elements in the numerical model, taking into account the necessary refinement of the mesh next to the crack front, Lin and Smith (1999) and Kurguzov (2016), a simplification of the geometry was considered. Only the central part of a T-welded joint is simulated, a slice of 20 mm width with boundary conditions that reproduce a plane state of deformation. It was considered the pre-existence of a semi-elliptical crack with a depth of 1.0 mm at the center of the slice. Given the symmetry of geometry and loading, only half of this slice was considered in the numerical model.

The base material used in this study was a medium strength steel, S355, in the form of plates with 12.5mm thickness. The welds were made by covered electrode process with weld metal in overmatching condition. T-joints weld specimens were produced from the main plates with low penetration fillet welded with an attachment of equal thickness. TIG post-weld treatment was performed at the weld toe. The weld leg length presented a medium value of 9 mm and the radii at the weld toe have a medium value of 6.25 mm, Ramalho et al. (2011).

For the mechanical characterization of the S355 steel in the elastic and plastic regime, were used the properties presented in Ramalho et al. (2018).

The initial mesh consisted of 2454 nodes and 12488 tetrahedral, full integration, linear elements. The element class was chosen considering the posterior use of the model to simulate the generation and growth of cracks. This structured mesh was generated in MSC Patran software.

In this initial mesh was generated the semi-elliptical pre-existing crack with 1 mm of depth and a superficial length of 4 mm. This initial crack was generated in MSC Marc software by a faceted surface, through a remeshing process. This model, at this stage with a mesh of 16006 nodes and 77482 tetrahedral elements, was subjected to three-point bending fatigue, with pulsating nominal load, -F, corresponding to a stress range at the weld toe of 215 MPa. Three different initial conditions were considered:

A. Without initial stress field;

B. With a tensile initial residual stress field generated by a compressive overload of -2.4*F;

C. With a compressive initial residual stress field generated by a traction overload of 3*F.

In order to evaluate the effect of the stress concentration caused by the preexisting crack, the propagation of a crack generated in a residual tensile stress field was also simulated, that is, the initial model, without crack, was subjected to the overload, which produced the residual stress field:

D. Without initial stress field;
E. With a tensile initial residual stress field generated by a compressive overload of -2.4*F;
F. With a compressive initial residual stress field generated by a traction overload of 3*F.

Subsequently, in these models, was generated a crack that was subjected to fatigue loading, by three-point bending, with pulsating nominal load, -F. The mesh refinement in these models is not so demanding, so the whole specimen (slice) was simulated without symmetry.

The loading by three-point bending was simplified through connections of the type REB2's, MSC Marc (2018) in order to reduce the model's number of elements. This rigid connection makes it possible to transmit the bending load applied at a remote node to a section closer to the region of analysis, the weld toe. This simplification of the model allows a significant reduction of the number of elements. The model is shown in Fig. 1.

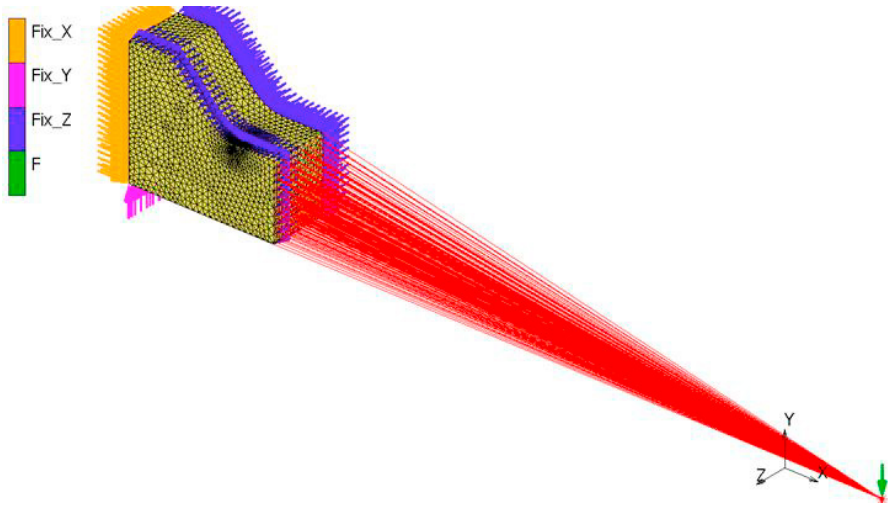

Fig. 1. Numerical model.

The overload causes plastic deformation at the crack front and in the weld toe. The plastic deformation causes a residual stress field in these regions. These stress fields are simulated in independent jobs. In these jobs, the overload is applied in quasi-static conditions, and the von Mises yield criterion is used to evaluate the plastic deformation, with an isotropic hardening rule. These residual stress fields are imputed in the crack growth simulations as initial conditions using the General Previous Analysis State condition.

From the analysis of experimental results of previous work, Ramalho et al. (2011), in which similar specimens are subjected to fatigue cracking, it was considered that the predominant propagation mode was Mode I and that the crack propagated in the transverse direction. However, in independent simulation, named simulation G, it was evaluated the direction of propagation using the Maximum Hoop Stress criterion, Hu et al. (2020).

The crack propagations was evaluated using the integration of Paris-Erdogan law (1), according to:

$$\Delta a = \int_{a_i}^{a_f} da \; = \; \int_{N_i}^{N_f} C\Delta K^m \, dN. \tag{1}$$

For the material propagation constants were used the values, C = 1.2288x10^{-8} and m= 2.6, with da/dN in mm/cycle and K in MPa.m$^{1/2}$, Ramalho et al. (2011).

The estimation of fatigue life including the effect of residual stresses may be done using different approaches. ΔK based approaches have been used by different authors to predict the effect of residual compressive stresses, Ruzek et al. (2012). Superposition techniques are often used when assessing the effects of a known residual stress field on fatigue crack propagation, Garcia et al. (2016). The superposition involves the computation of a stress intensity factor $(K)_R$ which is associated with the initial pre-existing residual stress field. The stress intensity factors due to pre-existing residual stresses and due to external loads are added.

In this work, the determination of the stress intensity factors was made using the 3D VCCT technique implemented in MSC Marc software. This native implementation uses the 3D VCCT formulation presented in Krueger (2004) for hexahedral mesh, adapted to the tetrahedral mesh. In this formulation each node of the crack front is treated as an 2D crack with an area of influence.

The initial semi-elliptical crack is propagated by fatigue, repeating the load sequence a number of times. After each sequence, crack is grown. For high cycle fatigue, the specified maximum growth increment, is scaled along the crack front. This scaling allows the determination of the shape of the crack front during growth. A maximum crack growth increment of $\Delta a_0 = 0.5$ mm was used, Kurguzov (2016). The scaling of this increment to each node on the crack front (Δa) is based on equation (2), Marc (2018).

$$\Delta a = \frac{\Delta a^{fat}}{\Delta a^{fat}_{max}} \Delta a_0 \,, \tag{2}$$

where Δa^{fat} is the growth increment for each crack-node in the crack front, calculated by the Paris-Erdogan law using the respective ΔK. To ensure that the crack fronts stay smooth, a smoothing scheme was used based upon running averages for the growth increments along the crack front.

In this approach the crack length increment, Δa0, was prescribed and the corresponding number of fatigue cycles, N, was calculated by the integration of Paris-Erdogan Law (1), assuming a constant value for the stress intensity factors, ΔK, along the increment of the crack.

3. Results and discussion

3.1. Residual stress fields

In Fig. 2 and Fig. 3 are presented the normal residual stresses on the x direction, σ_{xx}, generated by the overloads on the previous cracked models.

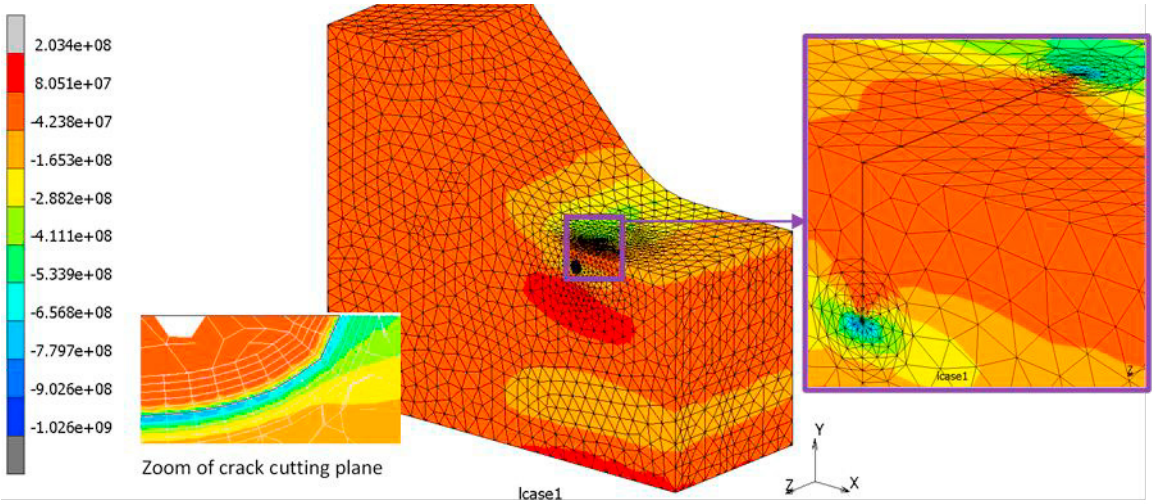

Fig. 2. Residual stress field, σ_{xx} [Pa], generated by traction overload.

In Fig. 2 it is possible to verify the existence of a field of residual compressive stresses along the entire crack front and at the weld toe, that extends over a relatively wide region (up to about 1.5 mm from the crack front). This residual stress field was generated by the tensile overload. The compressive stresses in the crack front reach the value of -900 MPa at the deeper region. Compressive stresses with lower values, up to -400 MPa, occurs in all the weld toe.

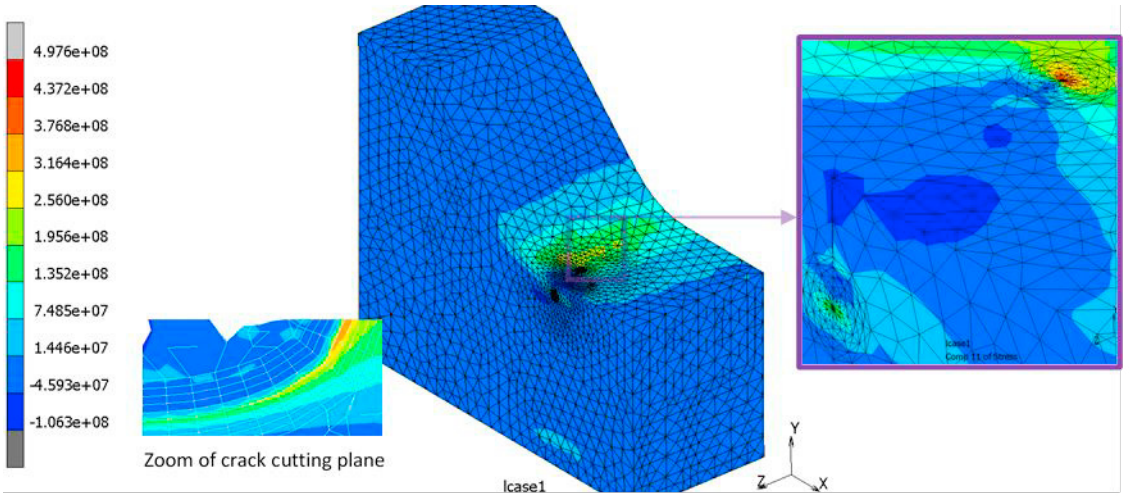

Fig. 3. Residual stress field, σ_{xx} [Pa], generated by compressive overload.

In Fig. 3 it is possible to verify the existence of a field of residual tensile stresses along the entire crack front and at the weld toe, that extends over a narrow region (up to about 0.5 mm from the crack front). In the deepest points of the crack front, after the narrow strip of tensile stresses, there are extensive regions with compression stresses that can reach -100 MPa. This residual stress field was generated by a compression overload. The tensile stresses at the crack front reach the value of 370 MPa near the surface. Tensile stresses with lower values occur in all the weld toe.

In Fig. 4 are presented the normal residual stresses in the x direction, σxx, generated by the overloads on non-cracked models.

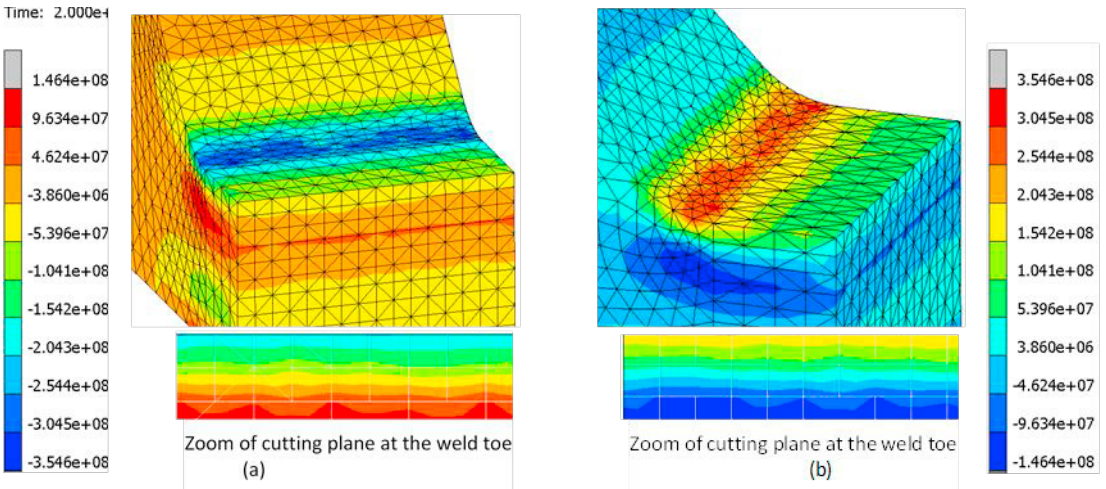

Fig. 4. Residual stress field, σ_{xx} [Pa]: (a) compressive overload; (b) traction overload.

In Fig. 4 (a) there is a residual compression stress field at the weld toe. Compression stresses up to about 0.8 mm in depth are noted. This residual stress field was generated by a tensile overload. The compressive stresses at the weld toe reach the value of -250 MPa.

In Fig. 4 (b) there is a residual tensile stress field at the weld toe. There are tensile stresses up to about 0.8 mm in depth. This residual stress field was generated by a compression overload. The tensile stresses at the weld toe reach the value of 200 MPa.

Fig. 5 shows the evolution of the crack front obtained with the simulations A, B and C.

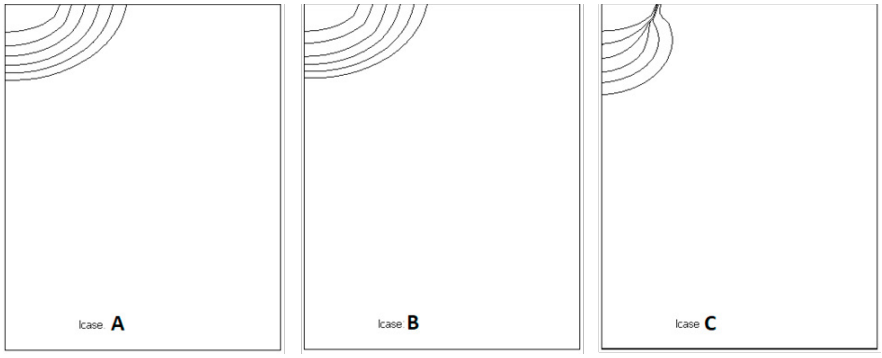

Fig. 5. Evolution of the crack front along the simulations A, B and C.

From the results presented on Fig. 5 we can draw the following considerations:

- The evolution of crack front along the crack growth in the simulation A, for the model without initial stress field, maintain its initial semi-elliptical shape;
- The evolution of crack front along the crack growth in the simulation B, for the model with initial tensile stress field, is similar to the simulation A, maintaining its initial semi-elliptical shape;
- The evolution of crack front along the crack growth in the simulation C, for the model with initial compressive stress field, it is completely different from the previous simulations. The crack is arrested at surface, and the propagation develops preferably in depth, occurring the tunneling effect.

The final configurations of the crack front in simulations D, E and F are presented in Fig. 6. The evolutions of the crack front along the simulations D, E and F are similar to the ones observed in simulations A, B and C, respectively. However, the effect of crack arrest at the surface in the simulation F are not so effective as observed in simulation C.

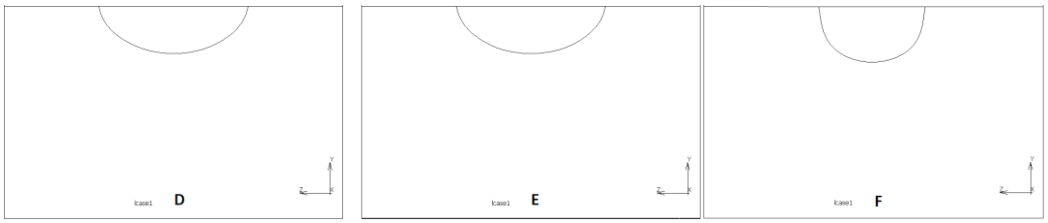

Fig. 6. Final crack front in simulations D, E and F.

In Fig. 7 are confronted the final configuration of the crack in simulation F, were the propagation occurs in mode I and perpendicular to the x axis, with a simulation performed in the same initial conditions but where the direction of propagation was obtained by the Maximum Hoop Stress criterion, simulation G.

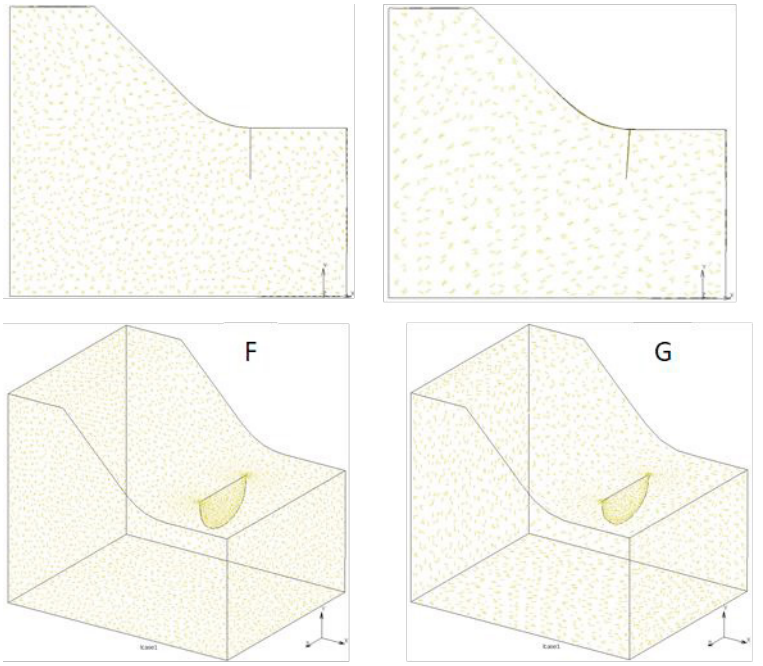

Fig. 7. Final crack in simulations F and G.

From the presented configurations, it appears that the final crack geometry is similar, with only a small rotation in the direction of the weld rib, in the case of propagation obtained by the Maximum Hoop Stress criterion, confirming the previous assumption that the predominant propagation mode was Mode I and the crack propagated mainly in the transverse direction, Ramalho et al. (2011).

In Fig. 8 are presented the fatigue results obtained in the various simulations.

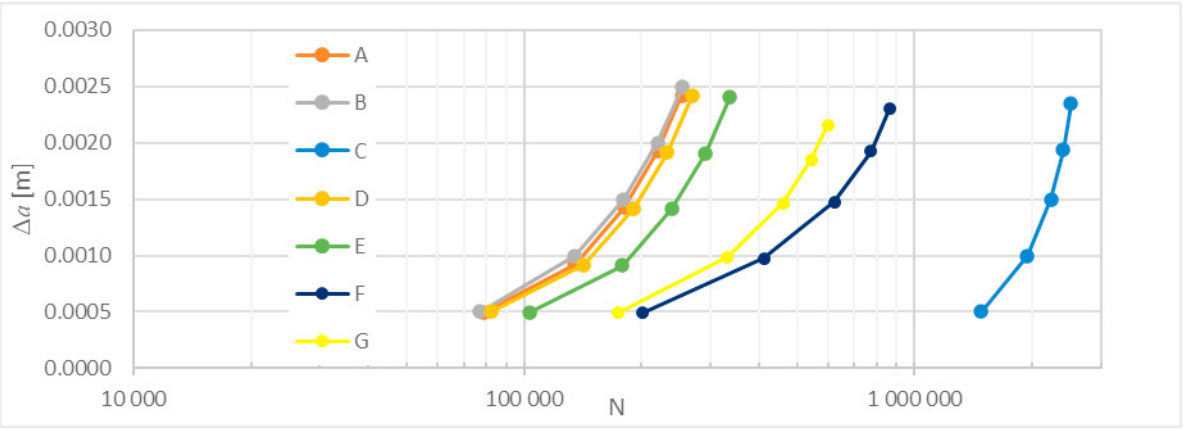

Fig. 8. Fatigue results.

From the fatigue results we can draw the following findings:

- The effect of tensile stress fields in the pre-cracked models (simulation B) is despicable, since the behaviour of crack growth is similar to the observed on the model without any initial stresses (simulation A);

- The effect of compressive stress fields in the pre-cracked models (simulation C) is very significant, with a great decrease in the crack propagation speed after overload;
- The effect of tensile stress fields in the models where the crack initiation occurs after the overload (simulation E), corresponds to a slight decrease in the crack propagation rate after overload, when compared to the model without any initial stresses (simulation D);
- The effect of compressive stress fields in the models where the crack initiation occurs after the overload (simulation F) is very significant, with a great decrease in the crack propagation rate after overload, however this effect is lower than in the pre-cracked model (simulation C);
- When the crack path is obtained by the Maximum Hoop Stress criterion (simulation G) it is considered the energy release of all modes of propagation, and the crack propagation rate is slightly higher than in mode I, propagating in in the transverse direction (simulation F).

The characteristics of propagation verified in the various simulations can be explained by the magnitude of the stress fields near the crack front and its redistribution as the crack grows. In Fig. 9 is shown the normal component in x direction of the stress field that occurs when the crack propagation is approximately 1 mm, $\Delta a \approx 1.0$ mm, for simulations C and E.

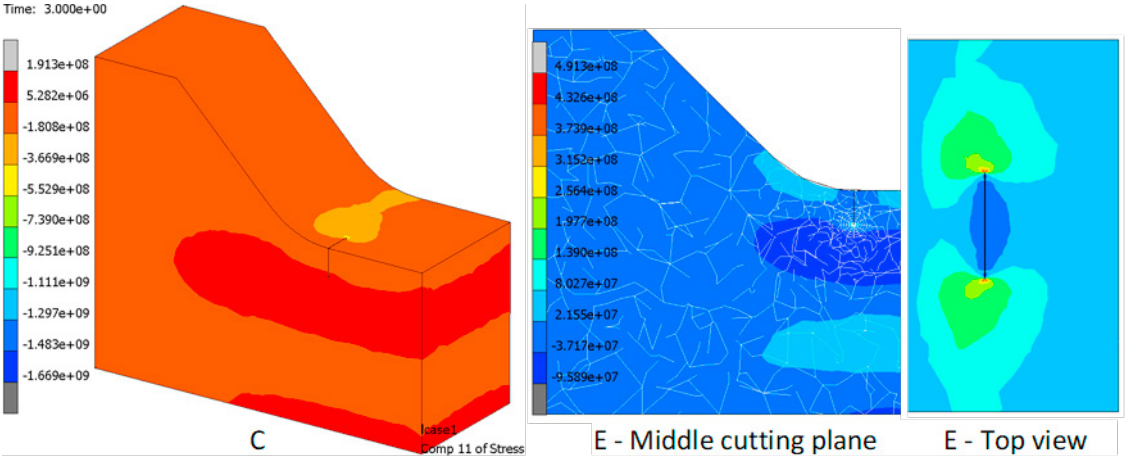

Fig. 9. Stress field, σ xx; , $\Delta a \approx 1.0$; Simulations C and E.

From these results are evident the compressive stresses at the crack front that occur at the surface of the specimen in simulation C, with magnitude of - 550 MPa, that are responsible for the crack arrest at this point, visible in the figure 5. The stresses at the deepest point are approximately zero, with tensile fields in its vicinity, promoting propagation in this direction and the tunneling effect.

On the other hand, in simulation E, it appears that at this stage of propagation, the stresses in the deepest crack front are slightly compressive, favoring the reduction of the propagation rate in this direction, while at the surface the tensile stresses favor the growth and the shallowing of the semi-ellipse.

The fatigue's lives obtained with the numerical simulation A were compared with the ones obtained by numerical integration of the Paris-Erdogan law (1) where the stress intensity factors are obtained the Mk factor proposed by Bowness and Lee (2000), included in BS 7910 standard. The results are shown in Fig. 10.

The solution proposed by Bowness and Lee (2000) give more conservative results, with higher crack propagation rates; when comparing the results of simulation A with the experimental results published in Ramalho et al. (2011), it appears that this simulation, using the VCCT, better fits the experimental results.

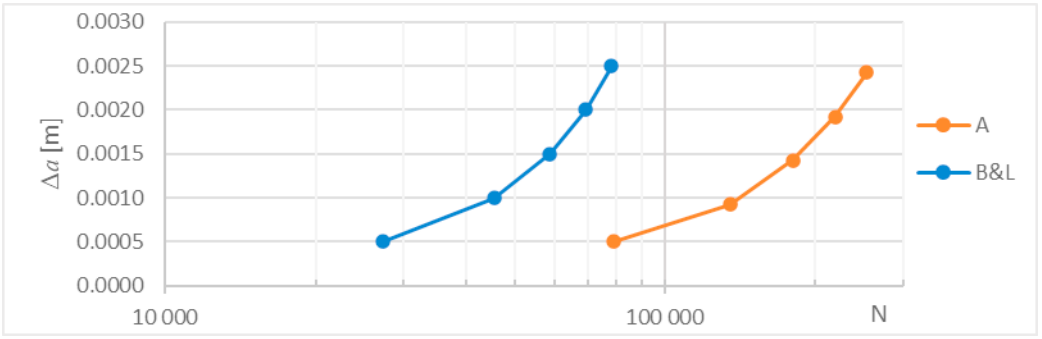

Fig. 10. Comparison between the solution obtained by VCCT and the one proposed by Bowness and Lee (2000).

4. Conclusions

The developed Finite Element Model reveals to be effective to predict the growth of cracks at the weld toe of a T-joint.

The developed Finite Element Model reveals to be effective to evaluate the influence of residual stresses generated by plastic deformation at the weld toe on the crack propagation speed.

The compressive stress fields generated by overloads on the cracks propagating in the weld toe of T-joints promote the crack arrest at the surface and tunneling effect on the crack growth.

The tensile stress fields generated by overloads on the cracks propagating in the weld toe of T-joints have a despicable effect on the crack growth.

When the stress fields are generated before the initiation of the crack, their effect on crack growth is less effective than the ones generated in pre-cracked specimens.

Acknowledgements

This research is sponsored by national funds through FCT – Fundação para a Ciência e a Tecnologia –, under the project UIDB/00285/2020.

References

Barsoum, Z., Barsoum, I., (2009). Residual stress effects on fatigue life of welded structures using LEFM. Engineering Failure Analysis, 16:1, 449-467.

Bikdeloo, R., Farrahi, G.H., Mehmanparast, A., Mahdavi, S.M., 2020. Multiple laser shock peening effects on residual stress distribution and fatigue crack growth behaviour of 316L stainless steel, Theoretical and Applied Fracture Mechanics 105, 102429.

Bowness, D., Lee, M.M.K., 2000. Prediction of weld toe magnification factors for semielliptical cracks in T-butt joints, Int J Fatigue 22(5), 369–87.

Garcia, C., Lotz, T., Martinez, M., Artemev, A., Alderliesten, R., Benedictus, R., 2016. Fatigue crack growth in residual stress fields, International Journal of Fatigue 87, 326–338.

Giglio, M., Lodi, M., 2009. Optimization of a cold-working process for increasing fatigue life, International Journal of Fatigue 31, 1978–1995.

Hu, Y., Song, M., Liu, J., Lei, M., 2020. Effects of stop hole on crack turning, residual fatigue life and crack tip stress field. Journal of the Brazilian Society of Mechanical Sciences and Engineering 42, 216.

Krueger, R., 2004. Virtual crack closure technique: History, approach and applications. Applied Mechanics Reviews, Vol. 57:2, 109-143.

Kurguzov, V.D., (2016). Selection of Finite-Element Mesh Parameters in Modeling the Growth of Hydraulic Fracturing Cracks, Journal of Applied Mechanics and Technical Physics, Vol. 57, No. 7, 1198–1207.

Lacarac, V., Smith, D.J., Pavier, M.J., Priest, M., 2000. Fatigue crack growth from plain and cold expanded holes in aluminium alloys, International Journal of Fatigue 22, 189–203.

Lin, X.B., Smith, R.A.,1999. Finite element modelling of fatigue crack growth of surface cracked plates. Part III: stress intensity factor and fatigue crack growth. Engineering Fracture Mechanics 63, 541-556.

Marc 2018. Volume A: Theory and User Information. User Documentation, MSC Software Corporation.

Okada, H., Higashi, M., Kikuchi, M., Fukui, Y., Kumazawa, N., 2005. Three dimensional virtual crack closure-integral method (VCCM) with skewed and non-symmetric mesh arrangement at the crack front, Engineering Fracture Mechanics 72, 1717–1737.

Ramalho, A.L., Antunes, F., Ferreira, J.A.M., 2020. Crack Growth In Simulated Residual Stress Fields On Tungsten Inert Gas Dressed Welded Joints – A 2D Approach. Anales de la Mecânica de la Fractura, 104-109.

Ramalho, A.L., Antunes, F., Nobre, T., Ferreira, J.A.M., 2018. Caraterização Mecânica do Aço S 355 a Temperatura Elevada, TEMM2018 – 1st Iberic Conference on Theoretical and Experimental Mechanics and Materials, 4-7 November, Porto, Portugal.

Ramalho, A.L., Ferreira, J.A.M., Branco, C.M., 2011. Fatigue Behaviour of T Welded Joints Rehabilitated by Tungsten Inert Gas and Plasma Dressing. Materials and Design 32:10, 4705-4713.

Ruzek, R., Pavlas, J., Doubrava, R., 2012. Application of indentation as a retardation mechanism for fatigue crack growth, International Journal of Fatigue 37, 92–99.

Shreyas, P., Trishul, M.A., 2014. Overview of research on Surface Mechanical Attrition Treatment (SMAT), International Advanced Research Journal in Science, Engineering and Technology, Vol. 1, Issue 4.

Wang, S., Li, Y., Yao, M., Wang, R., 1998. Compressive residual stress introduced by shot peening, Journal of Materials Processing Technology 73, 64–73.

Zeng, W., Liu, G.R., Jiang ,C., Dong, X.W., Chen, H.D., Bao, Y., Jiang, Y., 2016. An effective fracture analysis method based on the virtual crack closure – integral technique implemented in CS-FEM, Applied Mathematical Modelling 40, 3783–3800.

Zhao, X., Mo, Z.-L., Guo, Z.-Y., Li, J., 2020. A modified three-dimensional virtual crack closure technique for calculating stress intensity factors with arbitrarily shaped finite element mesh arrangements across the crack front, Theoretical and Applied Fracture Mechanics 109, 102695.